

## Statistics for ionospherically diffracted VHF/UHF signals

C. L. Rino and E. J. Fremouw

Stanford Research Institute, Menlo Park, California 94025

(Received May 22, 1972; revised November 27, 1972.)

In this paper a general characterization of the statistics for an ionospherically diffracted, monochromatic plane wave is presented. The main results are restricted to weak scatter, although two possible extensions that accommodate large phase perturbations and multiple scatter are discussed. A detailed discussion of the first-order statistics of amplitude is given. The general Gaussian distribution is discussed together with its Nakagami-distribution approximation and the log-normal distribution. By using a segment of ATS-3 satellite data recorded at Lima, Peru, we show equally good fits to Gaussian and log-normal distributions at least for the limited dynamic range available. The Nakagami distribution provides only a poor approximation. A transverse scale size of 600 m is inferred, which we believe is representative of the nearly linear dependence of the measured field's correlation distance on the Fresnel-zone radius.

### 1. INTRODUCTION

The statistics of transionospheric VHF-UHF signals have been studied extensively by communications engineers as well as geophysicists. Moreover, the same phenomena are observed in the scattering of light by turbulent air and of radio-star emissions by the solar wind. To date, however, few attempts have been made to fully utilize the statistical structure of homogeneous random fields as a basis for theoretical computations or experiment design.

In this paper we shall present a general characterization of the statistics for an ionospherically diffracted plane wave. The solution is the kernel of the more general case of an extended noise-like source, although that extension will not be pursued. Our approach follows the work of Bello [1971] who calculated the statistics of a signal scattered by the troposphere. The method was used in an early paper by Bowhill [1961]. More recently it was applied by Uscinski [1966, 1968] and Budden and Uscinski [1970].

Bello analyzed the voltage phasor at the receiving-antenna terminals. Following the more usual approach of geophysicists, we have chosen to analyze the complex field itself. This initially frees us from considering the effects of the receiving antenna (a spatial filter) and the receiver (a temporal filter).

We assume that the field is well approximated, at least locally, by a statistically homogeneous random field. The mean, or undeviated component, will be treated separately.

Let

$$E(x, y) = E_R(x, y) + iE_I(x, y) \quad (1)$$

represent the field. Since it is complex, a minimum of three correlation functions is required to specify the second-order statistics, namely, the spatial autocorrelation function of  $E_R$  and  $E_I$  and their cross-correlation. These, in turn, are most conveniently derived from the complex autocorrelation function of  $E$ ,

$$\begin{aligned} E_R(\delta x, \delta y) &\triangleq \langle E(x, y)E^*(x', y') \rangle \\ &= \langle E_R E_R' \rangle + \langle E_I E_I' \rangle + i(\langle E_I E_R' \rangle - \langle E_I' E_R \rangle) \end{aligned} \quad (2)$$

and the asymmetry autocorrelation function (Bello's terminology),

$$\begin{aligned} E_B(\delta x, \delta y) &\triangleq \langle E(x, y)E(x', y') \rangle \\ &= \langle E_R E_R' \rangle - \langle E_I E_I' \rangle + i(\langle E_I E_R' \rangle + \langle E_I' E_R \rangle) \end{aligned} \quad (3)$$

where  $\langle \cdot \rangle$  denotes ensemble average,  $\delta x = x' - x$ , and  $\delta y = y' - y$ . We have suppressed independent variables where confusion is unlikely. Note that  $\langle E_I' E_R \rangle$  can be derived from  $\langle E_I E_R' \rangle$ , so that only one of the two quantities need be specified.

For interpretation as well as computation, it is often more convenient to work in the spatial-fre-

quency domain. Most familiar is the real and non-negative spectral-density function,

$$\varphi(k_x, k_y) \triangleq F^{-1}(R_E) = \varphi_R + \varphi_I - 2 \operatorname{Im}(\varphi_{RI}) \quad (4)$$

where  $2 \operatorname{Im}(\varphi_{RI})$  is an asymmetric component and  $F^{-1}(\cdot)$  denotes the inverse two-dimensional Fourier transform, such that

$$\begin{aligned} F^{-1}(R_E) &= \int_{-\infty}^{\infty} \int_{-\infty}^{\infty} R_E(\delta x, \delta y) \\ &\cdot \{\exp[-i(k_x \delta x + k_y \delta y)]\} d\delta x d\delta y \quad (5) \\ \varphi_R &\triangleq F^{-1}(\langle E_R E_R' \rangle) \\ \varphi_I &\triangleq F^{-1}(\langle E_I E_I' \rangle) \\ \varphi_{RI} &= F^{-1}(\langle E_I E_R' \rangle) \end{aligned}$$

To determine the components of  $\varphi$  we use the complex spectral-density function

$$\varphi_B(k_x, k_y) \triangleq F^{-1}(B_E) = \varphi_R - \varphi_I + i2 \operatorname{Re}(\varphi_{RI}) \quad (6)$$

As with the cross-correlation function, the real and imaginary parts of the cospectral density  $\varphi_{RI}$  cannot be specified independently of one another.

We shall see in section 2 that  $R_E$  and  $B_E$  are easily computed for a weakly scattering medium. Moreover, the form of the results permits the determination of  $\varphi$  and  $\varphi_B$  by inspection. The results are independent of the particular spectral-density function for the scattering-medium irregularities and the incident-wave direction.

The complete statistical structure of the field can be determined from equations 2 and 3 if the statistics are Gaussian. We shall show that this is a good approximation for weak scattering. A general treatment of strong scattering is quite difficult. It is possible, however, to extend the results to accommodate large phase perturbations. The amplitude perturbation must still be small. These conditions are generally valid at VHF/UHF frequencies in the vicinity of the scattering medium.

Thus, if the complex phase is Gaussian, we would infer log-normal statistics for the field in the vicinity of the scattering medium. It is important to realize, however, that free-space propagation alters the statistics of the field. We discuss the simplest effect this could have on the observed statistics. A proper treatment of the general case must await accurate computations of the quantities we have discussed.

In section 3 we discuss in detail the first-order statistics of amplitude. This is of particular interest since amplitude statistics are the most readily ob-

served. We first consider amplitude statistics under the Gaussian hypothesis and the applicability of the approximate Nakagami distribution. Its use for VHF/UHF scintillation was suggested by *Bischoff and Chytil* [1969]. We then consider the different form that results if the amplitude statistics are log-normal.

To obtain analytic formulas for the necessary parameters we have assigned a Gaussian spatial autocorrelation function to the electron-density fluctuations as most other theorists have done. Unfortunately, the simple formulas that result can lead to erroneous interpretation of the data. Inferred spectral-density functions from amplitude data show a weighting of the spatial frequency components in inverse proportion to their wavenumber [*Rufenach*, 1971].

The effect is that the structure with size comparable to the Fresnel-zone radius  $(2\lambda z/\pi)^{1/2}$  dominates the data. This effect was inferred by *Rufenach* [1971]. It was demonstrated with a direct computation by *Matheson and Little* [1971]. The conclusion is that a single scale size at best leads to an incomplete specification of the statistics. A more useful parameter is the spectral index as used by both *Rufenach* [1971] and *Matheson and Little* [1971].

In section 4 we apply our results to analyze a segment of data from the synchronous satellite ATS-3 recorded at Lima, Peru. Using the simple formulas deduced by applying a Gaussian autocorrelation function, we infer a transverse scale size of 600 m. This result is somewhat larger than the usually accepted value [*Fremouw and Rino*, 1973], although it is easily understood in view of the aforementioned problem with the Gaussian autocorrelation function.

Our conclusion is that the amplitude statistics are non-Rician and poorly approximated by the Nakagami distribution. Moreover, the conditions for Rician statistics are unlikely to be achieved for the frequencies of interest here. The data are well fitted by density functions derived from Gaussian statistics when proper allowance is made for unequal amounts of power in the in-phase and phase-quadrature components as well as for their cross-correlation. This result has been anticipated by others [*Wernik and Liszka*, 1969] but not demonstrated.

Finally we show that over the dynamic range of the available data, the measured histograms are equally well fitted to a log-normal distribution. To perform a convincing separation between the two

possibilities (Gaussian versus log-normal) requires a very careful measurement, since the distinguishing features occur where the data are least certain. Future effort will be directed toward a more careful analysis of this aspect of the problem.

2. THE DIFFRACTION COMPUTATION

For a weakly scattering medium, the Booker-Gordon method can be applied to calculate the diffracted field. We shall use *Budden's* [1965] formula which has been rigorously derived by *Tatarski* [1969]. For an incident monochromatic plane wave  $E_0[\exp(-ik \cdot r)]$ , the diffracted field is given as

$$E(X, Y; z) = E_0[\exp(-ik \cdot r)][1 + \psi(X, Y; z)] \quad (8)$$

where

$$X = x - z \tan \theta \cos \varphi \quad (9)$$

$$Y = y - z \tan \theta \sin \varphi \quad (10)$$

An approximate expression for  $\psi$  is

$$\begin{aligned} \psi(X, Y; z) = & (k^2/2\pi) \int_{-L/2}^{L/2} \int_{-\infty}^{\infty} \int_{-\infty}^{\infty} \Delta n(x', y', z') \\ & \cdot ((\{\exp[-ikH'(X, Y)]\}/[(z - z') \sec \theta])) \\ & \cdot dx' dy' dz' \end{aligned} \quad (11)$$

where

$$\begin{aligned} H'(X, Y) \triangleq & \{(X - X')^2 + (Y - Y')^2 - \sin^2 \theta[(X \\ & - X') \cos \varphi + (Y - Y') \sin \varphi]^2\}/[(z - z') \sec \theta] \end{aligned} \quad (12)$$

In equation 11,  $L$  is the medium thickness,  $\Delta n$  is the deviation of the index of refraction from its mean value, and  $k = 2\pi/\lambda$  where  $\lambda$  is the wavelength. The coordinate system is shown in Figure 1. Note that  $X$  and  $Y$  are measured relative to the line-of-sight intercept in the plane of the measurement.

Since the frequencies of interest are well above the electron plasma frequency, we let  $\Delta n = -(2\pi r_e/k^2)\Delta N_e$ , where  $\Delta N_e$  is the deviation of the electron density from its mean value and  $r_e$  is the classical electron radius. To allow for slow variations of the statistics with altitude we let  $\Delta N_e' = \mu(z)\Delta N_e$ , where  $\mu(z)$  is a deterministic profile function [*Budden, 1965*]. We introduce the autocorrelation and spectral-density functions of  $\Delta N_e$  through the equations

$$\begin{aligned} & \langle \Delta N_e^2 \rangle_{\rho_{\Delta N_e}}(\delta x, \delta y, \delta z) \\ & \triangleq \langle \Delta N_e(x', y', z') \Delta N_e(x'', y'', z'') \rangle \\ & = \langle \Delta N_e^2 \rangle \iint \Phi(k_x, k_y; \delta z) \\ & \cdot \{\exp[i(k_x \delta x + k_y \delta y)]\} (dk_x/2\pi)(dk_y/2\pi) \end{aligned} \quad (13)$$

By substituting equations 8, 11, and 13 into equations 2 and 3, and making some straightforward approximations, we obtain our main results. We omit the details since the computations are similar to those performed by many other authors cited in the references. A simplification can be realized by omitting the deterministic factors in equation 8. That is, we first compute the second-order statistics of  $\psi$  in equation 8. The deterministic factors can be reintroduced as they are needed. The results can be compactly summarized as

$$\begin{aligned} \left\{ \begin{matrix} R_{\psi} \\ B_{\psi} \end{matrix} \right\} = & \pm [(\sigma_r^2 \sec \theta)/\kappa] \\ & \cdot \int_{-\infty}^{\infty} \int_{-\infty}^{\infty} \Phi(k_x, k_y, 0) \{\exp[iZg(k_x, k_y)]\} \\ & \cdot \{\exp[i(k_x X + k_y Y)]\} (dk_x/2\pi)(dk_y/2\pi) \end{aligned} \quad (14)$$

where

$$Z = [(\lambda \mp \lambda)z \sec \theta]/4\pi \quad (15)$$

$$g(k_x, k_y) = k_x^2 + k_y^2 + \tan^2 \theta (k_x \cos \varphi + k_y \sin \varphi)^2 \quad (16)$$

$$\kappa = \iint \Phi(k_x, k_y, 0) (dk_x/2\pi)(dk_y/2\pi) \quad (17)$$

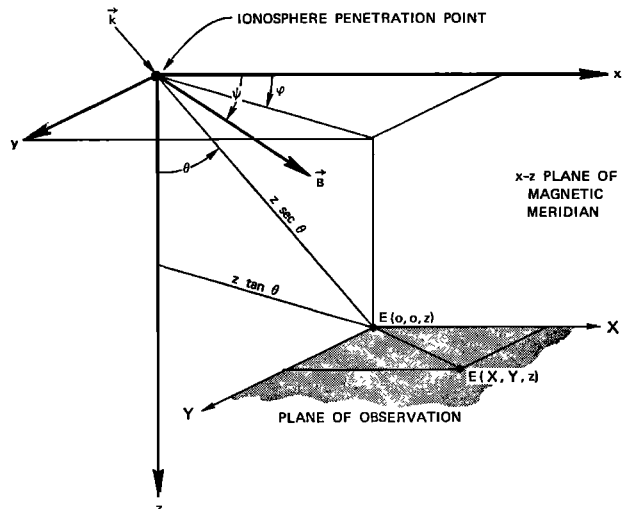


Fig. 1. Geometry for diffraction calculation.

$$\Phi(k_x, k_y, 0) = \int \Phi(k_x, k_y; \delta z) d\delta z \quad (18)$$

$$\sigma_T^2 = r_s^2 \lambda^2 (L \sec \theta) \mu^2(0) (\Delta N_s^2) \kappa \quad (19)$$

The upper sign in equations 14 and 15 is used for  $R_\psi$ , and the lower sign is used for  $B_\psi$ . Hence, the exponential involving  $g(k_x, k_y)$  does not appear in the  $R_\psi$  integral, and it is independent of  $z$ . The weak-scatter assumption requires that  $\sigma_T^2 \ll 1$ . The approximations made in deriving equation 9 are valid when  $(\lambda L \sec \theta) / \xi^2 \ll \xi^2 / 2$ , where  $\xi$  is the minimum irregularity scale size. For a more detailed discussion, see *Barabanenkov et al.* [1971].

Consider first the  $R_\psi$  integral. The result states that  $\Phi(k_x, k_y, 0)$  is the inverse Fourier transform of  $R_\psi$  in the  $X$ - $Y$  coordinate system. The final result actually depends only on difference coordinates. The special coordinate system simplifies the computation, however, provided that the aforementioned condition involving  $\lambda$ ,  $L$ , and  $\xi$  is valid. This result for  $R_\psi$  has been derived by other authors, e.g., *Cronyn* [1970].

The nature of the second-order statistics of  $E$  itself, as implied by equation 14, is most easily deduced from the behavior of  $R_\psi$  and  $B_\psi$  when  $X = Y = 0$ . With the normalization in equation 17,  $R_\psi(0, 0) = \sigma_T^2 \sec \theta$ . But, from equation 8, it follows that

$$\langle P_s \rangle \triangleq [\langle \mathbf{E}_s \cdot \mathbf{E}_s^* \rangle \cos \theta] / 2Z_0 = E_0^2 \sigma_T^2 / 2Z_0 \quad (20)$$

where  $\mathbf{E}_s = \mathbf{E}_0 [\exp(i\mathbf{k} \cdot \mathbf{r})] \psi$ , and  $Z_0$  is the intrinsic impedance of free space. Hence,  $\sigma_T^2$  is the ratio of the scattered power (per unit area) crossing a plane perpendicular to  $z$  to the total incident power (per unit area)  $E_0^2 / 2Z_0$  (see *Uscinski* [1968, equation 3.13]).

If we replace  $\sigma_T^2 \sec \theta$  in equation 14 by  $\langle P_s \rangle$ , we shall have computed scattered power (per unit area) crossing a plane perpendicular to  $z$ . Henceforth, this normalization will be used. The quantities of interest are

$$\sigma_R^2 \triangleq \langle E_R^2 \rangle = (1/2) \{ R_\psi(0, 0) + \text{Re} [B_\psi(0, 0; z)] \} \quad (21)$$

$$\sigma_I^2 \triangleq \langle E_I^2 \rangle = (1/2) \{ R_\psi(0, 0) - \text{Re} [B_\psi(0, 0; z)] \} \quad (22)$$

$$C_{RI} \triangleq \langle E_R E_I \rangle = (1/2) \text{Im} [B_\psi(0, 0; z)] \quad (23)$$

From equation 14 we deduce that  $\text{Re} [B_\psi(0, 0; 0)] = -R_\psi(0, 0)$ . Moreover, since  $\exp[iZg(k_x, k_y)]$  oscillates

rapidly for sufficiently large  $z$ , we deduce that  $\lim_{z \rightarrow \infty} B_\psi(0, 0; z) = 0$ .

We can identify three zones for the behavior of  $\sigma_R^2$ ,  $\sigma_I^2$ , and  $C_{RI}$  as functions of  $z$ . These are summarized in Table 1. The results show the power initially in phase quadrature with the undeviated component of the field. Ultimately it becomes equally divided between the in-phase and phase-quadrature components.

This result is a very old one, having been originally deduced by *Hewish* [1952]. It was demonstrated for a Gaussian autocorrelation function by *Bowhill* [1961]. It is important, however, to have a formulation independent of a particular spectral-density function. We shall see that the boundaries of the regions we have identified cannot be specified by a single scale size.

To complete the formal development we note, as others have, that with a loose application of the central-limit theorem, we can deduce a Gaussian limiting distribution for the statistics of  $\psi$ . It follows from equation 8 that the statistics of  $E$  itself are Gaussian, and we have the desired complete statistical description of the diffracted field. The main restriction is that  $\sigma_T^2$  be small compared to unity.

We conclude this section by briefly discussing two possible methods of extending the results to accommodate large values of  $\sigma_T^2$ . The simplest extension results from recognizing that  $1 + \psi$  in equation 8 is an approximation to  $e^\psi$ . The latter form results from an application of the method of smooth perturbations [*Tatarski*, 1969]. It is now fairly well established, however, that the method-of-smooth-perturbations solution is valid only when the amplitude fluctuation is small [*Barabanenkov et al.*, 1971].

Recall, however, that equation 14 describes the second-order statistics of  $\psi$ . Thus, the results in Table 1 apply to  $\psi$  if  $\langle P_s \rangle$  is replaced by  $\sigma_T^2 \sec \theta$ . It then follows from the method-of-smooth-perturbations form, equation 8 with  $1 + \psi$  replaced by  $e^\psi$ , that the amplitude fluctuation is small if  $\sigma_R^2$  is small. This could occur in the vicinity of the medium (small  $z$ ) even if  $\sigma_T^2$  itself is near unity. Thus, we expect the form to be accurate in the vicinity of the scattering medium, at least for typical conditions at VHF and UHF. In this instance we would deduce log-normal statistics for the field. That is, the logarithm of amplitude and phase are jointly Gaussian.

Now, however, we must explicitly perform the

TABLE 1. Behavior of  $\sigma_R^2$ ,  $\sigma_I^2$ , and  $C_{RI}$ 

	Near zone $z \sim 0$	Intermediate zone	Far zone $z \rightarrow \infty$
$\sigma_R^2$	$\sim 0$	Increasing	$\sim \langle P_s \rangle / 2$
$\sigma_I^2$	$\sim \langle P_s \rangle$	Decreasing	$\sim \langle P_s \rangle / 2$
$C_{RI}$	$\sim 0$	$\sim$ Maximum	$\sim 0$

diffraction calculation for the ensuing free-space propagation. The technique is straightforward in principle, but difficult in practice. Limiting cases for amplitude and phase statistics have been evaluated by many authors, most notably *Salpeter* [1967]. In general, the free-space propagation can be viewed as a filtering of the spatial-frequency content of  $E_R$  and  $E_I$ . The filters exhibit no sharp cutoff, but spatial frequencies beyond  $\pi/2\lambda z$  are attenuated.

To obtain some feeling for the possible effect on the statistics, we consider a theorem from communications theory. It states that the output statistics of a narrowband filter are asymptotically Gaussian as the bandwidth approaches zero [*Papoulis*, 1972]. Hence, if this mechanism is operative sufficiently far from the medium, we may observe Gaussian statistics even if the method-of-smooth-perturbations solution is applicable in the vicinity of the medium.

Finally, we mention the work of *Uscinski* [1968]. He applied the thin-layer result as a differential operator describing the scattering of a single spatial-frequency component. By integrating over all spatial frequencies and adjusting amplitudes so that energy is conserved, he obtained a system of integral equations for  $\varphi$  and  $\varphi_B$  that include the effects of multiple scatter. In that case, large amplitude fluctuations are permitted. Unfortunately, the equations are quite difficult to solve although they are well-suited for numerical computation.

### 3. THE FIRST-ORDER STATISTICS OF AMPLITUDE

To describe the first-order statistics of amplitude,  $A = (E_R^2 + E_I^2)^{1/2}$ , we must determine the probability-density function or the cumulative-density function. Once this is done we can easily compute the probability-density functions for  $A^2$  or  $20 \log_{10} A$ , depending on the particular application. From the statistics of the complex field developed in section 2, we can derive the joint probability-density function for  $E_R$  and  $E_I$ , say,  $P_{RI}(x, y)$ . Then,

$$P_A(a) = \int_0^{2\pi} a P_{RI}(a \cos \theta, a \sin \theta) d\theta \quad (24)$$

For completely general Gaussian statistics *Beckman and Spizzichino* [1963] have discussed  $P_A(a)$  in detail. We shall only summarize the important features of the general case here. The contours of equal probability for the total field are ellipses. A typical contour is shown in Figure 2. They are characterized by the variance along the  $\xi$  axis,  $\sigma_1^2$ , and the  $\eta$  axis,  $\sigma_2^2$ . In addition, we need to know the orientation angle  $\zeta$  since we measure quantities involving  $E_R$  and  $E_I$ .

To ensure energy conservation, we adjust the amplitude of the undeviated component in equation 8 so that  $\langle E^2 \rangle = E_0^2$ . We further simplify our results by normalizing the field to unity incident power. Then,  $\sigma^2 = \langle P_s \rangle / (E_0^2 / 2Z_0)$  is the fraction of the incident power that is randomized by the scattering medium. With this simplification we easily obtain the results.

$$\sigma^2 = \sigma_1^2 + \sigma_2^2 \quad (25)$$

$$|B| = \sigma_1^2 - \sigma_2^2 \quad (26)$$

$$1/2 \angle B = \zeta \quad (27)$$

where  $B \equiv B(0, 0; z)$  is given by equation 14 with a suitable renormalization.

One additional quantity is important, namely, the scintillation index  $S_4$  defined as the normalized standard deviation of  $A^2$ :

$$S_4^2 \triangleq (\langle A^4 \rangle - \langle A^2 \rangle^2) / \langle A^2 \rangle^2 \quad (28)$$

For Gaussian statistics *Nakagami* [1960] has derived the result

$$S_4^2 = 2\sigma^2(1 - \sigma^2)[1 + (|B|/\sigma^2) \cos 2(\zeta - \phi)] + \sigma^4[1 + |B|^2/\sigma^4] \quad (29)$$

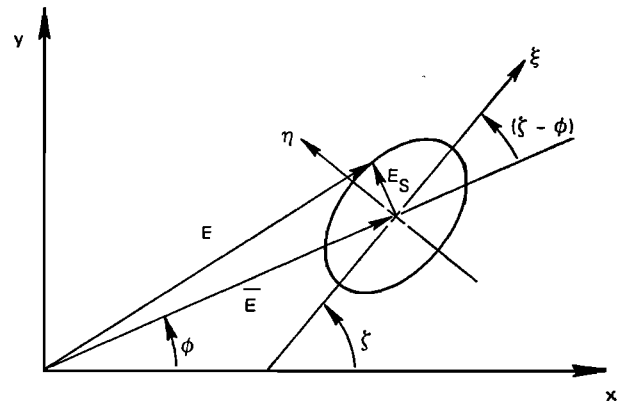


Fig. 2. Typical contour of equal probability for Gaussian statistics.

We note that  $S_4^2$  is given by a quadratic equation in  $\sigma^2$  with  $z$ -dependent coefficients. To make this explicit we write equation 29 as

$$S_4^2 = 2\sigma^2 g_1 + \sigma^4 (g_2 - 2g_1) \quad (30)$$

where

$$g_1 = 1 + (|B|/\sigma^2) \cos 2(\zeta - \phi) \quad (31)$$

$$g_2 = 1 + |B|^2/\sigma^4 \quad (32)$$

We also note that  $0 \leq S_4^2 \leq 2$ .

We now consider a particular spectral-density function, namely, the Gaussian form

$$\Phi(k_x, k_y, 0) = \pi^{3/2} a \xi^3 \exp \{ -k_x^2 (\xi\beta)^2/4 - k_y^2 \xi^2/4 \} \quad (33)$$

where

$$\beta^2 = a^2 \cos^2 \psi + \sin^2 \psi \quad (34)$$

The angle  $\psi$  is the magnetic dip angle at the ionosphere penetration point (see Figure 1),  $\xi$  is the transverse-scale size, and  $a$  is the axial ratio. Also, from equation 17,

$$\kappa = \sqrt{\pi} a \xi / \beta \quad (35)$$

It is then fairly straightforward to evaluate equation 14 to obtain the result

$$B = -\sigma^2 [(1 - \tan u_1 \tan u_2 \sec^2 \theta)^2 + (f_1 \tan u_1 + f_2 \tan u_2)^2]^{-1/2} \cdot \left\{ \exp \left[ \frac{1}{2} i \tan^{-1} \left( \frac{f_1 \tan u_1 + f_2 \tan u_2}{1 - \tan u_1 \tan u_2 \sec^2 \theta} \right) \right] \right\} \quad (36)$$

where

$$\tan u_1 = (2\lambda z \sec \theta) / [\pi(\xi\beta)^2]$$

$$\tan u_2 = (2\lambda z \sec \theta) / \pi \xi^2$$

$$f_1 = 1 + \tan^2 \theta \cos^2 \varphi$$

$$f_2 = 1 + \tan^2 \theta \sin^2 \varphi$$

For normal incidence,  $f_1 = f_2 = 1$ , and the result simplifies to

$$B_N = -\sigma^2 (\cos u_1 \cos u_2)^{1/2} \{ \exp [i(1/2)(u_1 + u_2)] \} \quad (37)$$

We shall now restrict our discussion to this special case.

It follows from equations 37, 26, and 27 that  $|\sigma_1^2 - \sigma_2^2| = \sigma^2 (\cos u_1 \cos u_2)^{1/2}$  and  $\zeta = (1/4)(u_1 + u_2) + \pi/2$ . In addition, from equations 31

and 32 we see that  $g_1 = 1 - (\cos u_1 \cos u_2)^{1/2} \cos (1/2)(u_1 + u_2)$  and  $g_2 = 1 + \cos u_1 \cos u_2$ . Now, as  $z$  varies from 0 to  $\infty$ ,  $u_1$  and  $u_2$  vary from 0 to  $\pi/2$ . Hence, when  $z = 0$ ,  $\sigma_1^2 = \sigma^2$ ,  $\sigma_2^2 = 0$ , and  $\zeta = \pi/2$ , in agreement with the behavior summarized in Table 1. As  $z \rightarrow \infty$ , the angle  $\zeta$  rotates from  $\pi/2$  to  $\pi$ , and  $\sigma_1^2$  and  $\sigma_2^2$  tend to  $\sigma^2/2$  from above and below, respectively.

The behavior of  $S_4^2$  with  $z$  depends on the magnitude of  $\sigma^2$  in general. For small  $\sigma^2$ , however, we can approximate equation 31 as  $S_4^2 \cong 2\sigma^2 g_1 = 4\sigma_R^2$ , which can be shown to be identical to the formula given by *Briggs and Parkin* [1963]. For oblique incidence, the formula derived from equation 36 is approximately equal to the Briggs-Parkin formula to zenith angles of approximately 20°. The discrepancy stems from the fact that Briggs and Parkin treated oblique incidence by effectively rotating the ionosphere normal to the propagation direction and increasing its thickness by the secant of the zenith angle. This technique greatly simplifies the calculations, but it is approximate.

We digress here briefly to consider the Nakagami probability-density function which is given by the formula

$$P_A(a) = \{2m^m a^{2m-1} / [\Gamma(m)]\} [\exp(-ma^2)] \quad (38)$$

The total intensity (power) is normalized to unity. In equation 38,  $m = (S_4^2)^{-1}$ . Because equation 38 depends only on a single readily measured parameter, it is an attractive candidate for  $P_A(a)$ . It has been applied to convert among various scintillation-index measures that have been used in practice [*Bischoff and Chytil*, 1969].

Nakagami found that equation 38 fit the distribution of amplitude fades observed on long-range HF (9.67 to 20.02 MHz) communication channels fairly well. He also showed [*Nakagami et al.*, 1953] that equation 38 can be derived as an approximation to the general Gaussian probability-density function for certain ranges of the parameter  $m$ .

For very strong scintillation, say, when  $\sigma^2 = 1$ , we have from equation 38 that  $\sigma_1^2 - \sigma_2^2 = (m^{-1} - 1)^{1/2}$ . The scintillation index  $S_4^2$  is then independent of  $\zeta$  and greater than unity. Nakagami showed that equation 38 is a good approximation to the true (Hoyt) distribution in this case. At the other extreme,  $S_4^2 \ll 1$ , Nakagami showed that equation 38 approximates a Rice distribution with  $\sigma_1^2 = \sigma_2^2 = (1/2) [1 - (1 - m^{-1})^{1/2}]$ .

We shall see, however, that the far-zone condi-

tions where a Rician probability-density function is accurate are rarely observed. Hence, while equation 39 may be more accurate than a strict Rician function, it cannot accurately represent the true function for typical scatter conditions at VHF and UHF.

To conclude this section we consider the form of the amplitude probability-density function if the field statistics are log-normal as discussed in section 1. The density function depends only on the variance of the real part of the complex phase perturbation  $\psi$ . Hence, the log-normal function is also easily applied in practice. Moreover, the scintillation index  $S_4^2$  takes the simple form

$$S_4^2 = \exp(4\sigma_R^2) - 1 \quad (39)$$

For log-normal statistics the maximum value of  $S_4^2$  is  $e^4 - 1$ . However, for small  $\sigma_R^2$ ,  $S_4^2 \cong 4\sigma_R^2$ , which is identical to the small  $\sigma^2$  form of equation 31. This simply verifies the fact that Gaussian and log-normal statistics are nearly identical for weak scatter, provided the Gaussian probability-density function includes all the parameters, namely,  $\sigma_R^2$ ,  $\sigma_I^2$ , and  $C_{RI}$ .

The log-normal probability-density function is important because it has been demonstrated to accurately represent the amplitude distributions observed in optics [Ochs and Lawrence, 1969] and in radio astronomy [Cohen et al., 1967; Young, 1971; Armstrong et al., 1972]. Armstrong et al. did, however, find difficulty in fitting the log-normal distribution over the entire range of their data. Thus, it is important to have a hypothesis other than a Rician distribution, which is generally a poor fit to the data.

#### 4. APPLICATION TO ATS-3 SATELLITE DATA

To test the theory developed in the previous sections, we have analyzed a segment of data from the synchronous satellite ATS-3 recorded at Lima, Peru. Two channels of data were received from antennas separated approximately 415 m along an E-W baseline. The frequency was 136.4 MHz. The data were recorded on December 17, 1969, from 0400 to 0440 UT. The scintillation was average (T. Golden, personal communication, 1971).

Histograms were computed on 1-min segments of the data with a 5-msec sampling interval. Hence, each histogram contained 12,000 samples. The intensity interval used in making the histograms was  $10^{-18}$  mw. The scintillation index  $S_4^2$  and the average

power were estimated on 25 consecutive segments. The average of the 25 estimates of  $S_4^2$  was 0.475 for channel 1 and 0.487 for channel 2. The standard deviation for both channels was less than 0.01.

Channels 1 and 2 should differ only in average power. Since the differences in the estimated values of  $S_4^2$  are on the order of the standard deviation, we have a good check on the consistency of our estimates. Our working parameters are the time average of power  $\langle P \rangle_T$  and the time average of power squared  $\langle P^2 \rangle_T$ .

If we assume Gaussian statistics,  $\langle P^2 \rangle_T$  and  $\langle P \rangle_T$  are not sufficient to determine the theoretical amplitude probability-density function. Thus, researchers have considered quantities involving higher moments, such as skewness [Salpeter, 1967]. With the spectral-density function specified, however, the theoretical results from sections 2 and 3 allow us to compute  $\sigma_R^2$ ,  $\sigma_I^2$ , and  $C_{RI}$  from  $\langle P^2 \rangle_T$  and  $\langle P \rangle_T$  alone.

We estimate  $S_4^2$  by using  $\langle P^2 \rangle_T$  and  $\langle P \rangle_T$  in equation 28. Then  $\sigma^2$  is determined as a function of  $g_1$  and  $g_2$  by solving equation 30. With  $\sigma^2$  determined, we evaluate equations 21, 22, and 23 as

$$\sigma_R^2 = (1/2)[\sigma^2 + \text{Re}(B)] \quad (40)$$

$$\sigma_I^2 = (1/2)[\sigma^2 - \text{Re}(B)] \quad (41)$$

$$C_{RI} = (1/2) \text{Im}(B) \quad (42)$$

with  $B$  given by equation 36. Numerically integrating equation 24 then gives a parameterized family of probability-density functions that can be compared to the measured histogram for a best fit.

Since the height of the scattering region,  $h$ , is fairly accurately known, we have chosen to fix this parameter together with the axial ratio,  $a$ , to produce a family of probability-density functions parameterized by the transverse scale size  $\xi_0$ . We used the values  $h = 350$  km and  $a = 10$  from an rms electron-density fluctuation model [Fremouw and Rino, 1973]. The resulting family is shown in Figure 3.

In Figure 4 we show the best fit to the data for the family of probability-density functions in Figure 3. The best fit is achieved for a 600-m transverse scale size. The statistical parameters are summarized in Table 2. To interpret these results, we have made a contour diagram of  $|B|/\sigma^2$  as a function of  $u_1$  and  $u_2$  (Figure 5). Recall that  $|B| = \sigma_1 - \sigma^2$ . Hence, large values of  $|B|/\sigma^2$  imply  $\sigma_1 \gg \sigma^2$ , which is characteristic of near-zone scatter. A small value of  $|B|/\sigma^2$  implies

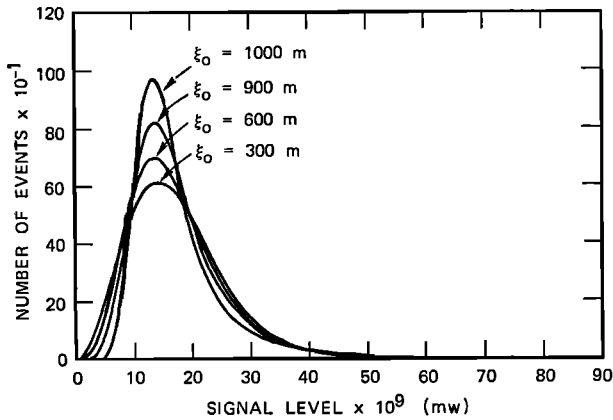


Fig. 3. Family of probability density functions for ATS-3 data in channel 1.

$\sigma_1 \approx \sigma_2$ , which is characteristic of far-zone scatter.

We have arbitrarily divided the behavior zones (Table 1) by the 0.8 and 0.4 contours. Also plotted are the  $u_1$  and  $u_2$  angles for the transverse-scale sizes used in Figure 3. Only for  $\xi_0 = 300$  m is the theoretical probability-density function well

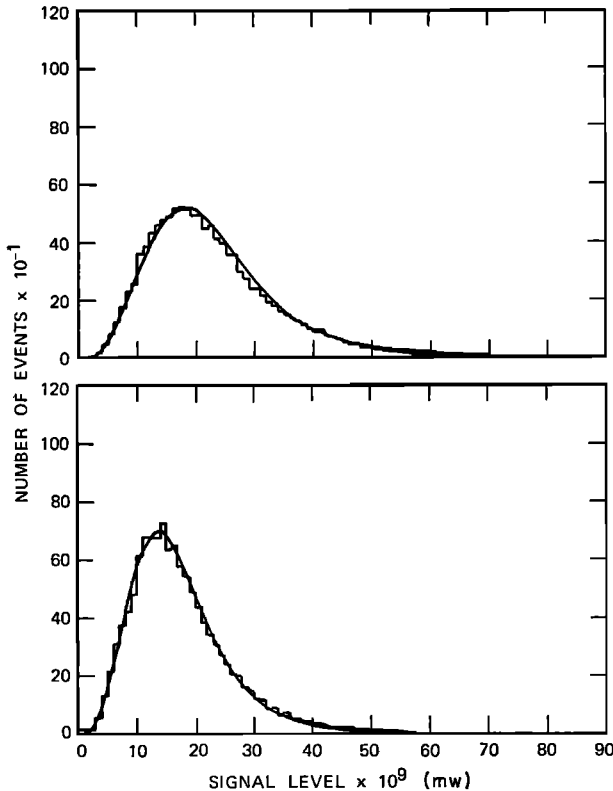


Fig. 4. Best fit to data for Gaussian statistics. The upper part is related to channel 2; the lower, to channel 1.  $\xi_0 = 600$  m.

TABLE 2. Computed parameters for ATS-3 data

Parameters	$\xi_0 = 600$ m	
	Channel 1	Channel 2
$S_4$	0.475	0.487
$\langle P \rangle$	$1.747 \times 10^{-12}$ mw	$2.307 \times 10^{-12}$ mw
$\sigma^2/\langle P \rangle$	0.239	0.250
$\sigma_R^2/\langle P \rangle$	0.0455	0.0475
$\sigma_I^2/\langle P \rangle$	0.194	0.202
$ B /\sigma^2$	0.717	—
$\zeta$	$105.00^\circ$	—

approximated by a Nakagami or Rice function. The best fit for  $\xi_0 = 600$  m occurs in the transition zone. This fact, however, is not coincidental.

The Gaussian spectral-density function is used mainly for analytical convenience. Spectral densities inferred from amplitude-scintillation data show a power-law behavior which weights the lower spatial frequencies in inverse proportion to their wavenumber. Ultimately, such a spectral density becomes singular [Rufenach, 1971]. There are, of course, physical mechanisms that prevent the catastrophe. Rufenach showed that the structure in the data is biased toward scale sizes on the order of the Fresnel-zone area. This is just the effect we observe in our own data.

In a recent paper Matheson and Little [1971] have performed theoretical calculations using a power-law spectrum. They approximate the spec-

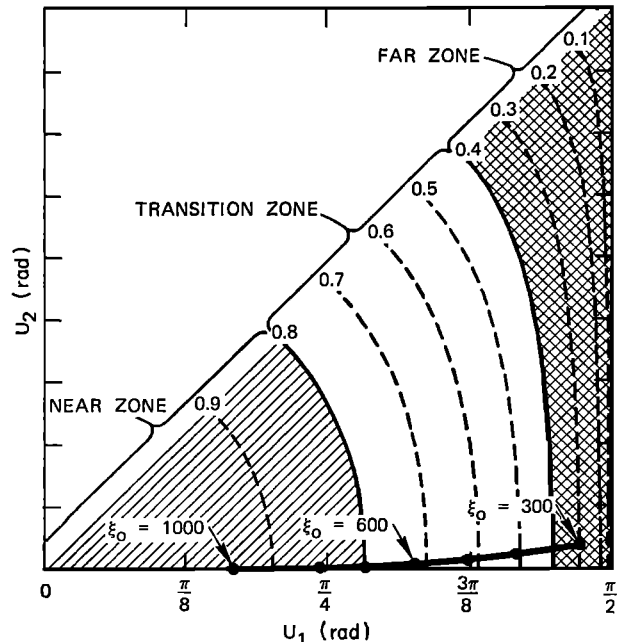


Fig. 5. Contours of constant  $|B|/\sigma^2$ .

trum of the amplitude fluctuations by the spectrum of the real part of  $E$  [Bowhill, 1961]. Thus, they compute what we called  $\varphi_R$  in the introduction. Their results are for normal incidence and isotropic irregularities, but they infer a linear relation between the correlation length and  $(\lambda z)^{1/2}$  for a spectral index between three and six. Since this range includes measured spectral indices for ionosphere scintillation, the phenomenon is well demonstrated by their results [Rufenach, 1971].

To test the log-normal-statistics hypothesis, we have fitted our data to a log-normal probability-density function. The single necessary parameter  $\sigma_R^2$  was determined by using the measured scintillation index  $S_4^2$  in equation 39. The result agrees to within a percent of the value given in Table 2, indicating that weak-scatter conditions are a good approximation. The result is shown in Figure 6.

The fit over the main portion of the histogram is not significantly different from that obtained with the Gaussian probability-density function. To identify the features that distinguish the log-normal and Gaussian statistics, we have plotted the theoretical curves

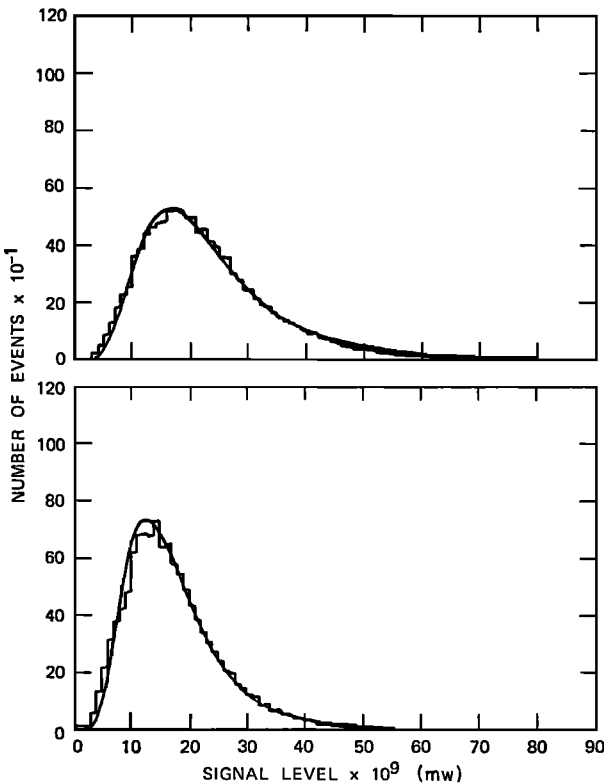


Fig. 6. Fit to data for log-normal statistics. The upper part is related to channel 2; the lower, to channel 1.

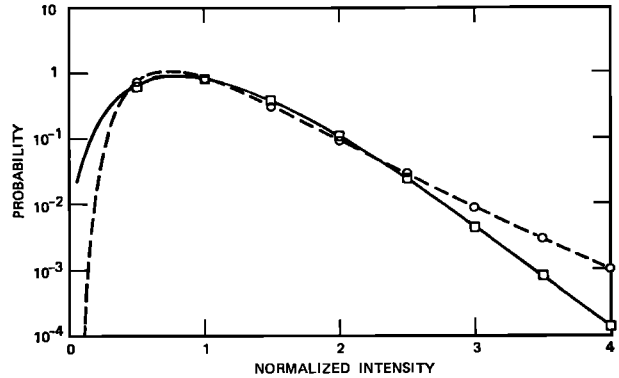


Fig. 7. Semilog plot of Gaussian —□— and log-normal —○— densities.

in Figures 4 and 6 on a semilog plot (Figure 7). The log-normal probability-density function rises more rapidly initially, then decays more slowly. The fact that the two curves are so close is somewhat surprising since the  $S_4$  index of .48 is not small. Ideally, data with an  $S_4$  index greater than .5 should be analyzed.

5. SUMMARY AND CONCLUSIONS

In section 2 we presented results, equations 8 and 14, that allow computation of the statistics, to second order, of the diffracted field for an incident monochromatic plane wave. The results are restricted to weak scatter, but they admit arbitrary incidence angles, and they do not depend on any particular form for the spectral-density function of the electron-density irregularities. Two possible extensions to allow strong scatter were also briefly discussed.

The behavior of the statistics to second order is characterized by the zero-lag functions  $\sigma_R^2$ ,  $\sigma_I^2$ , and  $C_{RI}$ . The general behavior is summarized in Table 1. For weak scatter the second-order statistics constitute a complete statistical description, since the scattered field is Gaussian. Moreover, if the variance of the real part of  $\psi$  from equation 8 is small, the results, with a proper interpretation, completely characterize the log-normal statistics in the vicinity of the scattering medium. The diffraction calculation for the free-space propagation, however, must be computed explicitly.

In section 3 we specialized the theory to the first-order statistics of amplitude. Log-normal statistics as well as Gaussian statistics were considered. The dependence of the  $S_4$  scintillation index typifies the differences. Equation 28 depends on  $\sigma_R^2$ ,  $\sigma_I^2$ , and  $C_{RI}$ , while equation 39 depends only on  $\sigma_R^2$ . We

also included a discussion of the Nakagami distribution which also depends only on a single parameter, the inverse of  $S_4^2$ .

Simple analytic formulas for  $\sigma_R^2$ ,  $\sigma_I^2$ , and  $C_{RI}$  can be obtained if a Gaussian spectral-density function (equation 32) is used in equation 8. The Gaussian function, however, does not adequately describe the spectral-density function inferred from amplitude scintillation data. The components are weighted in inverse proportion to their wavenumber. Hence, the spectral index, rather than a scale size, is the appropriate quantity to characterize the structure in the scattering medium. The effect is evident in the data analyzed in section 4.

We conclude that the Gaussian spectral-density function and the assumption of Gaussian statistics accurately describe the observed amplitude-probability density. The Nakagami distribution is a poorer approximation. For the data analyzed the  $\xi_0 = 300$  m (Figure 3) is closest to the Nakagami distribution. For systems applications the log-normal probability-density function is more accurate and more easily applied. The inferred scale size, however, gives little information about the irregularity structure of the medium itself.

The question of whether log-normal statistics are more appropriate than Gaussian statistics is important in verifying our understanding of wave propagation in a randomly irregular medium. We have shown, however, that very careful analysis is required to resolve this question. Previously, no realistic alternative has been applied in analyzing data.

The work presented here was undertaken initially to complement and extend the worldwide rms electron-density model discussed in *Fremouw and Rino* [1973]. The model was derived empirically from published scintillation indices. Thus, it depended on assumptions that were made about the first-order statistics in order to convert among the various scintillation indices reported.

We believe, on the basis of the results presented in this paper, that the model could be greatly improved by fully analyzing the amplitude statistics. Appropriate data are just becoming available, and future effort will be directed toward this goal. The results will be useful for communications-systems planning and evaluation as well as improving our understanding of the structure of the ionosphere.

*Acknowledgments.* The authors wish to thank Mrs. Dolores McNeil who did the computer programming. The ATS-3 satellite data were provided by Mr. Thomas Golden

of NASA. This research was supported in part by the National Aeronautics and Space Administration under contract NAS5-21551, and in part by the Defense Nuclear Agency under contract DASA-68-C-0104.

#### REFERENCES

- Armstrong, J. W., W. A. Coles, and B. J. Rickett (1972), Observations of strong interplanetary scintillation at 74 MHz, *J. Geophys. Res.*, **77**(16), 2739-2743.
- Barabanov, N., A. Kravtsov, S. M. Rytov, and V. I. Tamarski (1971), Status of the theory of propagation of waves in a randomly inhomogeneous medium, *Sov. Phys. Usp.*, **13**(5), 551-575.
- Beckman, P., and A. Spizzichino (1963), *The Scattering of Electromagnetic Waves from Rough Surfaces*, pp. 119-136, Pergamon, New York.
- Bello, P. A. (1971), A study of the relationship between multipath distortion and wavenumber spectrum of refractive index in radio links, *Proc. IEEE*, **59**(1), 47-75.
- Bischoff, K., and B. Chytil (1969), A note on scintillation indices, *Planet. Space Sci.*, **17**, 1059-1066.
- Bowhill, S. A. (1961), Statistics of a radio wave diffracted by a random ionosphere, *J. Res. Nat. Bur. Stand., Sect. D*, **65D**, 275-292.
- Briggs, B. H., and J. A. Parkin (1963), On the variation of radio star and satellite scintillations with zenith angle, *J. Atmos. Terr. Phys.*, **25**, 339-365.
- Budden, K. G. (1965), The amplitude fluctuations of the radio wave scattered from a thick ionospheric layer with weak irregularities, *J. Atmos. Terr. Phys.*, **27**, 155-172.
- Budden, K. G., and B. J. Uscinski (1970), The scintillation of extended radio sources when the receiver has a finite bandwidth, *Proc. Roy. Soc., Ser. A*, **A316**, 315-339.
- Cohen, M. H., E. J. Gundermann, H. E. Hardebeck, and L. E. Sharp (1967), Interplanetary scintillations, 2, Observations, *Astrophys. J.*, **147**, 449-466.
- Cronyn, W. M. (1970), The analysis of radio scattering and space-probe observations of small-scale structure in the interplanetary medium, *Astrophys. J.*, **161**, 755-763.
- Fremouw, E. J., and C. L. Rino (1973), An empirical model for behavior of average *F*-layer scintillation at VHF/UHF, *Radio Sci.*, **8** (this issue).
- Hewish, A. (1952), The diffraction of galactic radio waves as a method of investigating the irregular structure of the ionosphere, *Proc. Roy. Soc. London*, **214**, 494-514.
- Matheson, D. N., and L. T. Little (1971), Radio scintillations due to plasma irregularities with power law spectra: The interplanetary medium, *Planet. Space Sci.*, **19**, 1615-1624.
- Nakagami, M. (1960), The M-distribution: A general formula of intensity distribution of rapid fading, in *Statistical Methods in Radio Propagation*, edited by W. C. Hoffman, pp. 3-36, Pergamon, New York.
- Nakagami, M., S. Wada and S. Fijimura (1953), Some considerations on random phase problems, *J. Inst. Elec. Commun. Eng., Japan*, **S6**, 595-602.
- Ochs, G. R. and R. S. Lawrence (1969), Saturation of laser beam scintillation under conditions of strong atmospheric turbulence, *J. Opt. Soc. Amer.*, **59**, 226-227.

- Papoulis, A. (1972), Narrow-band systems and gaussianity, *IEEE Trans. Inform. Theory*, *IT-18*(1), 20.
- Rufenach, C. L. (1971), A radio scintillation method of estimating the small-scale structure in the ionosphere, *J. Atmos. Terr. Phys.*, *33*, 1941-1951.
- Salpeter, E. E. (1967), Interplanetary scintillations, 1, Theory, *Astrophys. J.*, *147*, 433-448.
- Tatarski, V. J. (1969), *Wave Propagation in a Turbulent Medium*, pp. 59-62 and 124-126, Dover, New York.
- Uscinski, B. J. (1966), The probability distribution of the wave field scattered by an irregular medium, *J. Atmos. Terr. Phys.*, *29*, 641-650.
- Uscinski, B. J. (1968), The multiple scattering of waves in regular media, *Phil. Trans. Roy. Soc. London, Ser. A*, *262*(1133), 609-643.
- Wernik, A. W., and L. Liszka (1969), On the amplitude distribution of scintillating radio signals from artificial satellites, *Ark. Geofys.*, *5*(34), 501-514.
- Young, A. T. (1971), Interpretation of interplanetary scintillations, *Astrophys. J.*, *168*, 543-562.